Comprehensive two-dimensional temperature-responsive × reversed phase liquid chromatography for the analysis of wine phenolics

Kristina Wicht[a], Mathijs Baert[a], Magriet Muller[b], Elena Bandini[a], Sonja Schipperges[c], Norwin von Doehren[d], Gert Desmet[e], André de Villiers[b], Frederic Lynen[a]*

a) Separation Science Group, Department of Organic and Macromolecular Chemistry, Ghent University, Krijgslaan 281-S4, B-9000 Ghent, Belgium.
b) Department of Chemistry and Polymer Science, University of Stellenbosch, Private Bag X1, ZA-7602 Matieland, South Africa.
c) Agilent Technologies, Hewlett Packard St 8, D-76337 Waldbronn, Germany.
d) Agilent Technologies, Netherlands BV, NL-4330 EA Middelburg, Netherlands.
e) Department of Chemical Engineering, Vrije Universiteit Brussel, Pleinlaan 2, B-1050 Brussel, Belgium

*Corresponding Author.

Tel: +32 (0) 9 264 9606; Fax: +32 (0) 9 264 4998. E-mail: frederic.lynen@ugent.be (F. Lynen)

Abstract

Phenolic compounds are an interesting class of natural products because of their proposed contribution to health benefits of foods and beverages and as a bio-source of organic (aromatic) building blocks. Phenolic extracts from natural products are often highly complex and contain compounds covering a broad range in molecular properties. While many 1D-LC and mass spectrometric approaches have been proposed for the analysis of phenolics, this complexity inevitably leads to challenging identification and purification. New insights into the composition of phenolic extracts can be obtained through online comprehensive two-dimensional liquid chromatography (LC×LC) coupled to photodiode array and mass spectrometric detection. However, several practical hurdles must be overcome to achieve high peak capacities and to obtain robust methods with this technique. In many LC×LC configurations, refocusing of analytes at the head of the ^{2}D column is hindered by the high eluotropic strength of the solvent transferred from the ^{1}D to the ^{2}D, leading to peak breakthrough or broadening. LC×LC combinations whereby a purely aqueous mobile phase is used in the ^{1}D and RPLC is used in the ^{2}D are unaffected by these phenomena, leading to more robust methods. In this contribution, the combination of temperature-responsive liquid chromatography (TRLC) with RPLC is used for the first time for the analysis of phenolic extracts of natural origin to illustrate the potential of this alternative combination for natural product analyses. The possibilities of the combination are investigated through analysis of wine extracts by TRLC×RPLC-DAD and TRLC×RPLC-ESI-MS.

Keywords

- Comprehensive two-dimensional liquid chromatography (LC×LC)
- Temperature-responsive liquid chromatography (TRLC)
- Analyte refocusing
- Phenolics
- Flavonoids
- Wine

Highlights

- Temperature-responsive × reversed phase comprehensive LC×LC-UV-MS for natural product analysis
- Separation of phenolics through simplified 2D method development
- TRLC×RPLC-UV can be performed on a commercial system in a fully automated manner including a new column selectivity and temperature programming in ^{1}D.

1. Introduction

Due to its versatile nature allowing physical separation of most classes of solutes, excellent reliability, reasonable speed, and because it can be combined with a variety of detectors, sample preparation approaches, or other separation techniques, High Performance Liquid Chromatography (HPLC) has become a central technique in chemical analysis. Nevertheless, the analysis of samples containing more than 50 analytes usually results in at least partially overlapping peaks in conventional HPLC [1]. Various approaches such as ultra-high pressure HPLC (UHPLC), the introduction of core-shell particles, and the development of monolithic phases have led mainly to faster analyses, with some improvements in peak capacity in one-dimensional LC (1D-LC). While implementation of long columns in combination with high-temperature LC and/or elevated pressures offers the most possibilities to enhance the peak capacity in 1D-LC [2–4], by far the largest gains in peak capacity can be obtained in (optimized) comprehensive two-dimensional liquid chromatography (LC×LC) [1,5,6]

After the first introduction of LC×LC in 1978 [7], and its more recent commercialization, the technique has increasingly proven to be a powerful tool for the analysis of complex samples [8]. As the full first dimension (^{1}D) effluent is collected in fractions and transferred through a high-pressure switching valve for separation on a second column [9], two optimally orthogonal selectivities become exploitable, offering high separation power and increased peak capacities [8,10,11]. This recurrent transfer of fractions in an automated way characterizes the online comprehensive mode. If higher peak capacities need to be achieved, at the cost of higher analysis times, offline or stop-flow approaches can be used [12,13]. In offline LC×LC, fractions of the ^{1}D effluent are collected and injected onto a ^{2}D column without a valve interface, whereas in stop-flow mode the ^{1}D flow is stopped following transfer of each fraction to the second dimension (^{2}D) column. Despite its benefits, the theoretically achievable gain in peak capacity of online LC×LC is hard to obtain in practice due to ^{1}D undersampling, suboptimal orthogonality, and analyte refocusing problems, which are issues interlinked with every step of the method development process, such as the chosen separation modes, column dimensions, the mobile phase compositions, flow rates, and injection volumes. One of the most relevant experimental hurdles is the effective transfer of fractions from the ^{1}D to the ^{2}D, which is hampered by solvent incompatibility or the use of solvents of too high eluotropic strength[14]. This leads to band broadening in the ^{2}D or even complete analyte breakthrough [1], reducing peak capacities and hindering robust implementation and method repeatability [15]. This phenomenon is common for some of the most used separation combinations such as NPLC×RPLC, HILIC×RPLC, GPC-SEC×RPLC, and to a lesser degree also RPLC×RPLC [1].

To reduce these effects, a decrease of the ^{1}D fraction volume transferred to the second dimension is pursued by miniaturization [16,17], reduction or splitting of the flow rate [12,18], by dilution with a weaker solvent [19,20], or by complete exchange of the ^{1}D effluent via e.g. vacuum evaporation [21] or using trap columns instead of the common loop interface [20]. However, most of these modifications affect detection sensitivity due to dilution issues, sample loss, decreased sample loading capacity, incomplete analyte recovery or more complicated method development [8,14,15,20,22]. The development of the Active Solvent Modulation (ASM) valve has allowed circumvention of these issues to some extent, at the cost of a minor increase in modulation time [15]. However, a few combinations of separation modes inherently allow for complete refocusing of analytes at the ^{2}D column head, for example aqueous SEC [14], IEC [8], or temperature-responsive chromatography (TRLC) [23], which are commonly used in combination with RPLC in ^{2}D [23,24]. SEC, however, is limited by lower separation efficiency (making it practically inadequate for small molecule analysis), and IEC requires ionic solutes and high non-volatile salt concentrations in the mobile phase, complicating subsequent hyphenation to MS in ^{2}D. By contrast, TRLC allows for reversed-phase type retention and separation of neutral organic molecules under the, for LC×RPLC, optimal purely aqueous separation conditions in ^{1}D.

Temperature-responsive stationary phases are based on smart polymers coupled to silica particles. Retention is governed by changes in solubility of the polymer in water as a function of temperature. As a consequence, this offers a tunable separation and retention based on hydrophobicity in purely aqueous media [23,25–28]. TRLC has thus far been mainly based on Poly (*N*-isopropylacrylamide) (PNIPAAm) immobilized on silica. This polymer undergoes a phase transition at the so-called lower critical solution temperature (LCST), whereby

below the LCST the polymer is soluble in water at any given polymer:solvent ratio, while above this value it becomes insoluble, in this way forming an apolar layer on the silica surface. For PNIPAAm, this reversible transition occurs around 32°C [23,25,29,30]. In past research, TRLC has been used to separate parabens, steroids, sulfonamides, peptides, and pesticides, etc. in 1D-LC [25,31–34]. In 2017, TRLC was for the first time used in 2D-LC as a pre-treatment column for the heart-cut analysis of biomolecules [35]. Recently, we introduced proof-of-principle studies illustrating the potential of TRLC×RPLC in comprehensive 2D-LC [23,24]. First, it was demonstrated that due to the use of water as a mobile phase, basically unlimited volumes of eluent can be transferred from the first to the second dimension with near-perfect peak refocusing, giving perspective for simplified modulation in comprehensive 2D-LC [23]. In a recent study, TRLC×RPLC was used for impurity determination in pharmaceutical analysis using temperature-programming in state-of-the-art LC×LC instrumentation [24]. In the present work, PNIPAAm-based TRLC×RPLC is for the first time coupled online to mass spectrometry and used for the analysis of natural product extracts, specifically the analysis of wine polyphenols.

Polyphenols are secondary plant metabolites, produced in response to stress factors like UV irradiation, and are especially known for their influence on food characteristics, such as color and taste [36–38]. Additionally, their antioxidant properties and prophylactic and therapeutic potential are of interest, as the role of oxidative stress is increasingly being investigated in diseases such as cancer and cardiovascular diseases [39–42]. In addition to their natural occurrence, polyphenols are often added to food or cosmetics to increase the product shelf-life. Modern techniques are used for identification and quantification of these micronutrients [37] in different matrices, where LC-MS or LC-high resolution MS (LC-HRMS) became the workhorses in the field [36–38,43]. The complexity of natural product polyphenol extracts is not only a consequence of the large number of compounds present, but also the fact that they cover a broad chemical space in terms of structural diversity, polarity, and molecular mass (<150 Da for phenolic acids to >30000 Da for polymeric compounds), while occurring at vastly different concentrations (from µg/kg to hundreds of mg/kg) [37,43,44]. Therefore, online, offline, and stop-flow LC×LC methods are increasingly being used for enhanced quantitation or MS-based structural elucidation [12,17,45]. As summarized in recent literature [6], the most used configuration for the analysis of polyphenols is RPLC×RPLC, followed by either HILIC×RPLC or RPLC×HILIC and to a lesser extent NPLC×RPLC [6,12,36,37,46–48]. The aqueous mobile phases applied in TRLC allow for a relatively straightforward implementation of LC×LC, and therefore show great potential for improving 2D-LC analysis of polyphenols.

2. Experimental

2.1 Reagents and materials

Acetonitrile (ACN, HPLC grade) was obtained from Sigma-Aldrich (Steinheim, Germany). Milli-Q grade water was purified and deionized in-house with a Milli-Q plus instrument from Millipore (18.2 mΩ) (Bedford, USA). Formic acid (FA) was purchased from Acros (Geel, Belgium). Small molecular weight phenolic standards were obtained from Sigma-Aldrich ((+)-catechin hydrate (≥98%), (-)-epicatechin (≥90%), gallic acid, quercetin (≥95%), (+)-rutin hydrate (94%)), vanillic acid (97%)), Fluka AG (caffeic acid (97%), naringin (≥95%)) or TCI Europe (kaempferol hydrate (>97%), trans-resveratrol (>99%)). The first dimension TRLC column (100×2.1 mm, 5 µm d_p, 100 Å) was obtained by reversible addition-fragmentation chain-transfer (RAFT) polymerization of NIPAAm followed by immobilization on aminopropyl silica (for more information, see the supplementary data section S1). The structure of the temperature-responsive stationary phase is displayed in Figure S1. In the second dimension, a Zorbax Eclipse Plus C18 RRHD column was used (50×3 mm, 1.8 µm d_p, 95 Å) (Agilent Technologies, Waldbronn, Germany).

2.2 Sample preparation

The stock solutions of the low molecular weight phenolic standards were prepared at 1 mg/mL in pure MeOH or 50:50 MeOH/H_2O (v/v) in case of vanillic acid, gallic acid and caffeic acid. The one-dimensional work was performed with individual solutions at a concentration of 200 µg/mL for kaempferol, quercetin, and resveratrol and 100 µg/mL for all other standard solutes. The stock solutions were thereby diluted with a premixed solution of 50:50 MeOH: H_2O (v/v) to their final concentrations in the samples before analysis. To remove unwanted

anthocyanins, and to avoid matrix-effects or co-elution with e.g. polymeric tannin fractions, phenolic extracts from a young South African red wine (Stellenbosch, 2019) were prepared. Therefore, 100 mL of the wine were extracted three times with 100 mL diethyl ether. The combined ether fractions were subsequently evaporated under reduced pressure at room temperature until less than 1 mL remained. The remaining liquid was reconstituted to 1 mL with MeOH and stored in the freezer. The final sample was diluted 1:5 in ACN prior to analysis, in accordance to the procedure described by Muller et al. [19]. The samples were filtered through 0.45 µm PTFE-filters (Millipore).

2.3 Instrumentation

Measurements were performed using the 1290 Infinity II 2D-LC System controlled by the OpenLab CDS ChemStation Edition software (C.01.08[210], Agilent Technologies, Waldbronn, Germany). This includes two binary pumps, a vial autosampler, and a 2-position/8-port valve mounted to a valve drive interface equipped with two (non-standard) 200 µL loops. To allow for inverse temperature gradients, a multicolumn thermostat, with two InfinityLab Quick-Connect heat exchangers (0.12 mm ID, 1.6 µL) for solvent pre-heating in the ^{1}D and ^{2}D were incorporated into the multicolumn thermostat. Detection was carried out with two diode array UV detectors containing a nano-flow cell in the ^{1}D (path length 10 mm, volume 1 µL) and a max-light cartridge cell in the ^{2}D (path length 60 mm, volume 4 µL). UV-VIS spectra were recorded between 200 and 600 nm (80 Hz). As a second detector in the ^{2}D, an ion trap MS$^{(n)}$ (LCQ™ Thermo Finnigan, San Jose, CA, USA) equipped with an electrospray ionization source was used, controlled by Xcalibur™ 2.0. LC raw data was converted to a data matrix using GC image R1.9b6 software (GCimage, Lincoln, U.S.A.) and contour plots were constructed using Origin Software (OriginPro 8.5, OriginLab Corporation). 3D plots and contour plots of the total and extracted ion chromatograms (for MS-based compound identification) were processed with python code (version 3.8) and PyCharm (Community Edition 2020.2.3 by JetBrains). Peak capacity and surface coverage were calculated using Microsoft Excel 2016 and MATLAB Software R2019b (The Mathworks, Natwick, USA).

2.4 One-dimensional methods

In all the described 1D and 2D analyses, 5 µL sample volumes were injected. The mobile phase consisted of Milli-Q water containing 0.1 vol-% FA. DAD detection was performed at 210, 254, 280, and 360 nm. Van Deemter analysis (Supplementary info S2) was performed with epicatechin, vanillic acid, caffeic acid, and resveratrol at 45 and 15°C at 0.025, 0.05, 0.1, 0.2, 0.5, and 0.75 mL/min in triplicate (%RSD of the retention times in S2, Table S1). For the construction of Van't Hoff plots all 10 solutes were analyzed once, at a constant flow rate of 0.1 mL/min, in the isothermal mode at 11 different temperatures in steps of 5-degree intervals from 0 to 50°C.

2.5 Two-dimensional methods

The ^{1}D separations were performed on a TRLC column (100×2.1 mm, 5 µm d_p, 100 Å), at an isocratic flow of 0.1 mL/min H_2O with 0.1 vol-% FA. An inverse temperature gradient was applied with the static air oven on the ^{1}D column (0-30 min: 45°C, 30.1 min: 0°C). The second-dimension column (Zorbax Eclipse Plus C18 RRHD 50×3mm, 1.8 µm, 95 Å) was operated at 50°C at a flow rate of 2.6 mL/min. A mobile phase composed of A: H_2O+ 0.1% FA (v/v) and B: ACN with 0.1% FA (v/v) was used in the gradient mode as outlined below. The modulation time t_m was set to 0.96 min, the gradient time t_g was 0.7 min, leaving 0.26 min for the re-equilibration of the ^{2}D column. The 8-port valve was equipped with two 200 µL loops (custom-made by Agilent Technologies, Waldbronn). DAD detection was performed at 254, 280, and 360 nm. The gradient applied in the first dimension was: 0% B from 0-220 min; 0–50% B in 220–230 min; 50-100% B from 230- 231 min; 100% B from 231-235 min. The gradient conditions used for the second dimension were: 1–45% B in 0–0.68 min; 45–100% B in 0.68–0.69 min; constant 100% B from 0.69-0.70 min, 1% B from 0.71 to 0.96 min. Repeatability data for three non-consecutive injections of the wine sample are given in the supplementary section S3. The ^{2}D effluent was split (1/10) prior to the UV detector such that 0.26 mL/min was directed towards the MS. UV absorbance data was recorded between 200 and 600 nm at 80 Hz acquisition rate. The LCQ MS$^{(n)}$ was equipped with an electrospray ionization source operated in negative ionization mode. The MS$^{(1)}$ mass range was set from 100 to 700 amu. The sheath gas flow (N_2) was operated at 60 and the auxiliary gas flow was set to 20. The spray voltage was 4.5 kV and the capillary was heated at 250°C. Collision-induced dissociation was operated at 8V to avoid the formation of clusters. The acquisition time was 240 min. The reconstructed total ion chromatograms and

extracted ion chromatograms for the identified compounds are given as 3D or 2D plots in the supplementary information, section S4 - S6. Peak capacity was calculated following usage of a peak detection algorithm from Peters et. al., [49]. A detailed explanation is provided in the supplementary information section (S7).

3. Results and discussion

3.1 Investigation of the retention behavior of common natural phenolic compounds in TRLC

Phenolic compounds are aromatic in nature and comprise one or more hydroxyl functionalities, ether bridges, or carboxylic groups which can be esterified. They often occur as glycosides or can form larger oligomeric structures. The (semi-) polar nature of polyphenols makes them particularly suitable for TRLC analysis under purely aqueous conditions in the first dimension of a comprehensive 2D-LC setup. To assess whether the TRLC separation mode is indeed suitable for the separation of phenolics while allowing satisfactory (and controllable) retention, acceptable elution times, and tunable selectivity, several representative standards, covering a relatively broad molecular space, were selected that can commonly be found in phenolic extracts from natural products. The standards used were selected to cover a range of polyphenol classes, including: flavonols (kaempferol, rutin and quercetin), flavanols (catechin and epicatechin), flavanones (naringin) and non-flavonoid compounds such as stilbenes (resveratrol), hydroxybenzoic acids (vanillic acid and gallic acid), and hydroxycinnamic acids (caffeic acid). The structures of these selected standard compounds are represented in Figure 1.

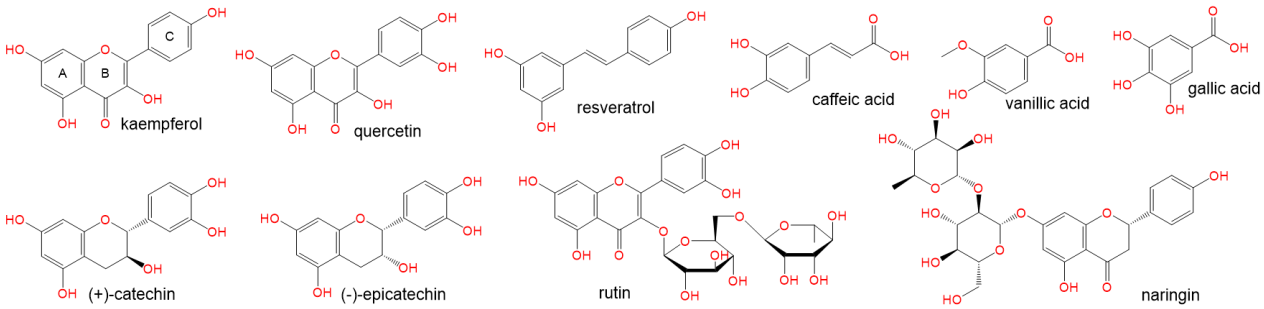

Figure 1: Structures of the phenolic standards used for the 1D method development.

To evaluate the influence of temperature on the retention of each standard, their retention was measured at 11 temperatures ranging from 50 to 0°C at a flow rate of 0.1 mL/min. The results are summarized in the van't Hoff plot presented in Figure 2a, where ln(k) is plotted against $^{1}/_{Temperature\ (Kelvin)}$. LogP values of the solutes are displayed in brackets behind the compound name in Figure 2a, taken from pubchem.com. While resveratrol has the highest logP value, it elutes earlier than kaempferol and quercetin, confirming what was already described in earlier TRLC work [25]: while retention increases on both TRLC (PNIPAAm) and RPLC (C18) columns based on an increase of hydrophobicity within a linear series of a compound family, the retention mechanisms differ for analytes depicting different polarity and functional groups [25]. Polar functionalities on relatively hydrophobic molecules can lead to increased retention in TRLC in comparison to RPLC [23], leading to selectivity differences and as such potentially higher orthogonality. Together with epicatechin, the rather large, glycosylated flavonoids naringin and rutin hydrate show the least retention, being the most hydrophilic. Interestingly, the steric difference of (-)-epicatechin and (+)-catechin resulted in an almost twice as high retention factor of the latter at 50°C. A further interesting observation is that an inversion in elution order takes place between kaempferol and quercetin below the LCST at around 20°C, resulting in higher ln(k) values for quercetin at low temperatures. The polymer chains are collapsed on the silica surface at a higher temperature and expanded in the aqueous mobile phase at low temperature, which might allow for more interaction with the additional hydroxyl group of quercetin, while hydrophobic interactions dominate at higher temperatures (leading to higher retention of this solute). The acids (caffeic-, vanillic- and gallic acid) are also well retained in TRLC due to the use of a low pH in the mobile phase comprising 0.1% formic acid. For visualization of the temperature-responsive effect, Figure 2b shows the retention time shift for the compound with the highest retention at high temperatures, kaempferol. This figure also demonstrates that the temperature dependency

depicts a gradual change rather than an "on-off" switch, enabling for example the use of reverse temperature gradients as a tool for compound elution. The retention factor (k) for kaempferol changes from 171 at 50°C to 22 at 0°C at a flow rate of 0.1 mL/min with a mobile phase consisting of H_2O + 0.1 vol-% formic acid, corresponding to an almost 8-fold decrease. Note that a slight increase in retention is observed from 15°C to 0°C. This is because this temperature range is below the relevant transition zone between the apolar and polar orientations of the polymer. Hence, in this temperature bracket, the normal thermodynamic behavior in HPLC (whereby retention increases with decreasing temperature) is dominant. Consequently, the lowest retention for kaempferol is obtained at 15°C, whereby a 10-fold decrease in retention compared to the analyses at 50°C is obtained.

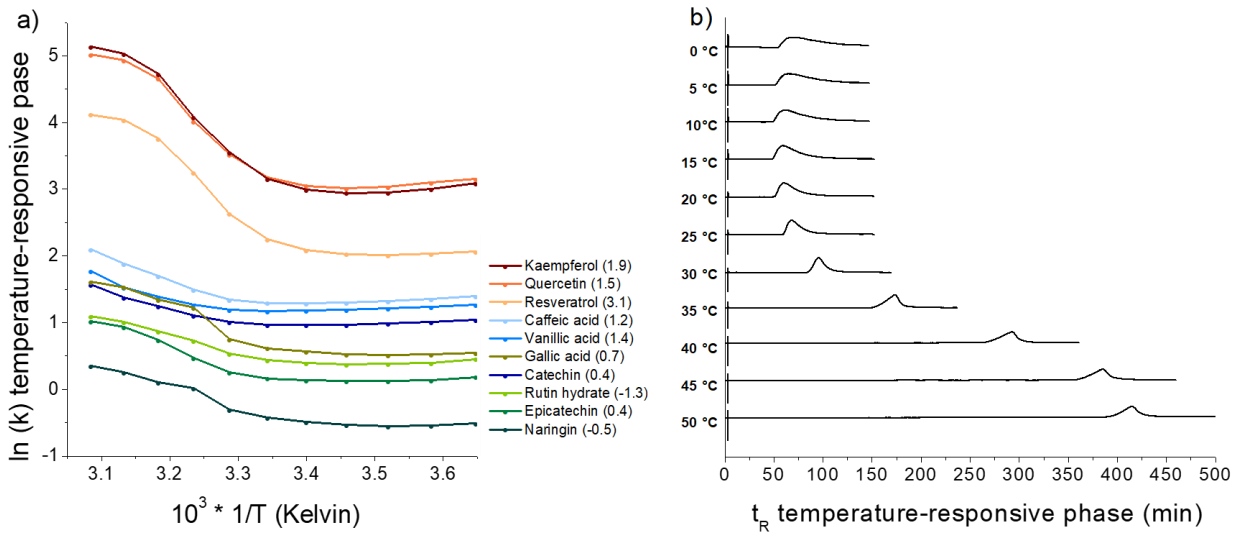

Figure 2: a) Van't Hoff plot of 10 different phenol standards at 0.1 mL/min H_2O + 0.1% v/v formic acid for temperatures ranging from 0-50°C in steps of 5°C. The TRLC column dimensions are 100×2.1mm, 5 µm, 100 Å. LogP values taken from pubchem.com are given in brackets behind the compound name b) Presentation of the increase of retention as a function of temperature shown for kaempferol under these conditions.

In TRLC the optimal efficiency is currently lower compared to state-of-the-art RPLC. However, this is not necessarily prohibitively problematic in LC×LC because relatively broad peaks in the first-dimension limit first dimension under-sampling and allow longer ^{2}D analysis times and therefore peak capacities. The rationale in TRLC×RPLC is that for this combination the limitations in ^{1}D efficiency is outweighed by the enhanced peak refocusing, simplicity of interfacing, and alternative selectivity it offers, as outlined in earlier work [23,24] and further for polyphenols in the present study. To obtain information on the peak broadening and ensuing peak volumes in TRLC, and on the performance of the specific TRLC columns developed for this work, plate height data were measured as a function of the flow rate. The corresponding Van Deemter curves were constructed for several representative solutes (epicatechin, vanillic acid, caffeic acid, and resveratrol) at temperatures below and above the transition temperature of PNIPAAm and are presented in Figure S2. The test solutes were selected to cover analytes in the low, medium, and high retention range and different flavonoid and non-flavonoid compound classes. The data illustrates that at the optimal velocity plate heights of ~20 µm are obtained, which is 2x higher compared to what can be obtained on C18 based RPLC on the same particle size [24,25,27]. This lower efficiency is related to the slower mass transfer in the (thicker) stationary phase, the in-house packing of the columns and due to the size dispersity of the aminopropyl silica used. The columns depicted optimal velocities around 0.2 mm/s (25 µL/min) [25] at 45°C. At temperatures below the LCST, the polymers are expanded, which detrimentally affects plate heights. However, because retention is obtained above the LCST, in practice TRLC is mainly performed above the LCST whereby the temperature is gradually lowered to reduce retention.

3.2 Optimization of conditions for the comprehensive two-dimensional analysis of phenolic compounds

The most important benefit of TRLC×RPLC is that the purely aqueous nature of the first TRLC dimension allows for complete refocusing at the head of the second-dimension column, independent of the transferred volume and hence of the loop size and the flow rate used in TRLC. This approach also avoids the pernicious necessity to miniaturize the internal diameter of the first dimension in LC×LC relative to the second-dimension column, which may lead to easily overloaded (^{1}D) columns and less sensitivity due to dilution. It is noteworthy that alternative LC×LC combinations for the analysis of phenolics may involve offline or stop-flow hyphenation to overcome such issues [12]. In this work, online LC×LC was used with passive modulation to transfer all fractions to the ^{2}D. While many combinations of ^{1}D flow rates, loop volumes and ^{2}D modulation times could be chosen due to the flexibility of TRLC×RPLC, a flow rate of 0.1 mL/min was selected in the ^{1}D, which corresponds to a higher than optimum velocity, but provides shorter analysis time. However, the analysis time was also strongly influenced by the application of the inverse temperature gradient in the static air oven of the system. Due to the thermal mass of this device, cooling from 45 to 0°C required about 60 min, as estimated based on the ^{1}D pressure signal (shown in Figure 3, purple line) which stabilized at the lowest temperature (and highest ΔP value) after this period. The second dimension was operated under fairly conventional state-of-the-art LC×LC conditions, using a Zorbax Eclipse Plus C18 RRHD column (50×3 mm, 1.8 µm d_p, 95 Å) at a flow rate of 2.6 ml/min. These column dimensions and particle type allow for relatively high flow rates, while still providing reasonable resolution even under the high linear velocities required in the ^{2}D. Further, the column was found to provide excellent stability performance over extended LC×LC operation times. The gradient of 1-45% ACN was chosen as it led to successful occupation of the separation space by the phenolic compounds in wine [19]. The obtained ^{2}D retention time repeatability of less than 0.7% (Supplementary info S3) and the absence of wrap-around in the ^{2}D suggest appropriate method conditions were selected. The modulation time and the loop volume were set at 0.96 min and 200 µL, respectively. These were both selected such as to allow for optimal ^{2}D analysis time without causing undersampling of the ^{1}D effluent. These method conditions result in a loop filling of 48%. It was advised, to fill loops to not more than 50% of the loop volume to avoid analyte loss due to the parabolic flow profile of the mobile phase in narrow loops [1]. An advisable filling volume of 50 – 80% dependent on the acceptable level of sample loss was further confirmed via simulations and practical work [50]. Due to the limited coiling of the loop and the relatively high ^{1}D flow rate, a conservative approach in loop filling volume was chosen. The ^{2}D column effluent was split (1/10) after the ^{2}D column to ensure compatibility with the ESI-MS detector [37]. Retention time repeatability (%RSD) for selected compounds can be found in the supplementary information (S3), for three injections of the wine sample. As a comparison, a measurement was performed keeping the 1D column isothermal at low temperature (0°C) to investigate lowest analysis times for the wine analysis (supplementary info S8). The overall analysis time was reduced by about 30 min, which roughly corresponds to the 30 min at temperatures above the LCST, which are applied in the here presented and optimized methods to assure best resolution and higher retention for the compounds early eluting in TRLC.

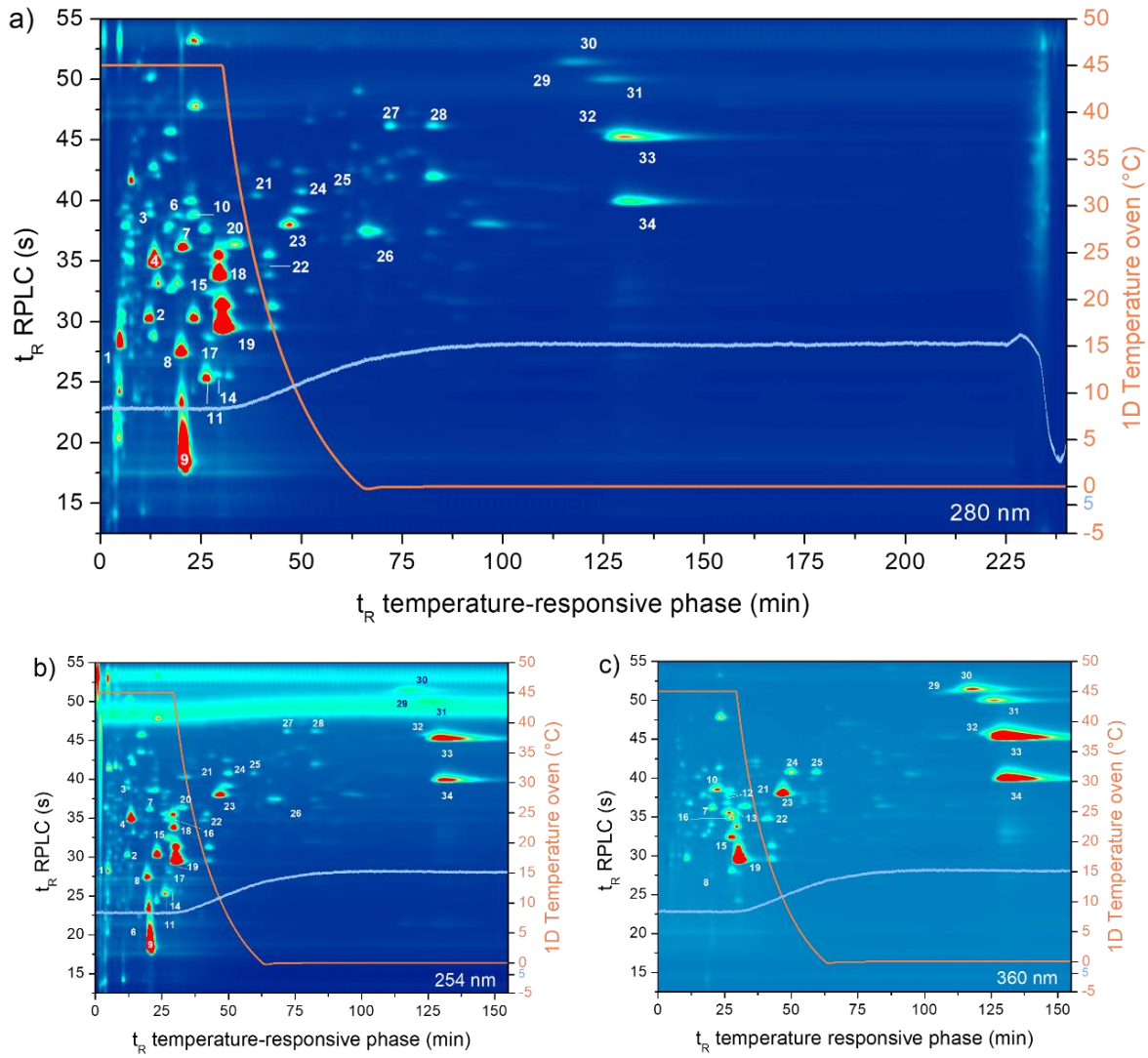

Figure 3: Contour plots obtained by TRLC×RPLC separation of the phenolic fraction of a young South African red wine at (a) 280 nm, (b) 254 nm and (c) 360 nm. The first dimension was performed using a reversed temperature gradient from 45 to 0°C at 30 min, indicated by the orange signal. The experimental pressure signal in the first dimension is shown by the light blue line as indication of actual column temperature change. Peak numbers correspond to Table 1 and represent peak identification via MS, literature research, and UV spectra.

3.3 TRLC×RPLC-UV-MS analysis of phenolic compounds extracted from wine

To assess the ability of the TRLC×RPLC setup to analyze natural products, ether extracts of a young red wine were prepared to concentrate the phenolic compounds of interest, and to remove anthocyanins and higher molecular weight polyphenols such as tannins. Even though MS (and ideally MS/MS) is ultimately necessary to identify phenolic compounds in complex natural mixtures, the benefits offered by the much-enlarged separation space obtained by TRLC×RPLC separation prior to the UV and MS detection can be observed in the contour plots represented in Figure 3. It is also evident from this figure that neither 1D TRLC nor RPLC separation would allow complete separation of all phenolics present in the ether extract for compound identification. Considering the observed complexity of the sample, direct analysis by ESI-MS would prove of little benefit and would only allow tentative identification of the more concentrated solutes depicting unique (fragment) masses, while providing little to no insight into absolute or relative concentrations of the phenolic solutes. This is due to the large differences in ionization efficiencies of organic molecules and matrix effects occurring for large numbers

319 of compounds covering a large concentration range in the electrospray source. Hence the physical separation
320 as obtained allows for more facile analysis of solutes by MS and also by UV/DAD. The latter offers e.g. easier
321 visual insight into families of solutes. This can e.g. be illustrated through the UV spectra of flavonols which are
322 distinct, while MS can only differentiate e.g. the glycosides of quercetin and kaempferol, when high-collision
323 energy *collision* induced dissociation (CID) is an option [37]. As polyphenols of different classes are
324 characterized by distinct UV/VIS spectra, a wide wavelength range (200-600 nm) was recorded to assist in the
325 detection, identification, and peak purity assessments. Several corresponding, and for phenolic solutes relevant,
326 contour plots were extracted at 280 nm (flavanols, procyanidines, flavanones), 254 nm (hydroxybenzoic acids),
327 and 360 nm (flavonols, flavones) (Figure 3a, b, and c, respectively)[37,51]. Also note that in the TRLC×RPLC-
328 ESI-MS combination only volatile mobile phase additives are used in both dimensions.

329 34 compounds were assigned based on the MS (and UV) data (Table 1, Figure 3), of which 17 were flavonols
330 (the aglycones myricetin, quercetin, kaempferol, syringetin, laricitrin and isorhamnetin, as well as eleven of
331 their glycosylated derivatives), two flavanols (epicatechin, catechin), three flavanonols (dihydromyricetin,
332 dihydrokaempferol and dihydroquercetin), four stilbenes (cis- and trans-piceid, cis- and trans-resveratrol) and
333 three B-type procyanidins. Additionally, the hydroxybenzoic acid derivatives syringic acid and gallic acid, as
334 well as the hydroxycinnamic acids fertaric acid, p-coumaric acid, and caffeic acid were also identified. Note that
335 anthocyanins were not detected because neither the extraction nor the separation protocol were optimized for
336 these solutes (typically requiring e.g. 5% formic acid to allow effective RPLC separation [52]). Compounds were
337 tentatively identified based on their online UV spectra, relative RPLC retention [19] and MS molecular ion [19]
338 and fragmentation data (no MS/MS data available) compared to literature [19,41,61–63,53–60].

339 Table 1: Tentative identification of the phenolic compounds in wine by TRLC×RPLC-DAD-MS: A) flavonols, B)
340 flavonol-glycosides, C) dihydroflavonols (flavanonols), D) stilbenes, E) flavanols, F) hydroxybenzoic acids and
341 derivates G) hydroxycinnamic acids, H) procyanidins. Deprotonated $[M-H]^-$ ions and fragmentation patterns
342 were mainly compared to Muller et. al. and other sources for confirmation of fragmentation patterns [13,19,61–
343 64,53–60]

	No.	Compound	t_R ^{1}D TRLC (min)	t_R ^{2}D RPLC (s)	Theoretical monoisotopic mass (Da)	Exp. mass $[M-H]^-$ (m/z)	MS/MS Fragments m/z negative mode	Fragments confirmed by literature
H	1	Fertaric acid	4.80	28.20	326.26	325.0		
E	2	Epicatechin	12.48	30.22	290.08	289.1	245, 203, $[2M-H]^-$: 579	[19,56–59]: 245 [19]: 203 [56]: 579
D	3	Cis-/trans-piceid	12.48	38.86	390.08	389.1	227	[19]: 227
F	4	Syringic acid	13.44	34.86	198.05	197.1	124, 169	[19]: 124, 169
	5	(Epi-) gallocatechin	16.32	19.99	306.07	305.0	179	[58]: 179
D	6	Cis-/trans-piceid	19.20	38.78	390,13	389.2		
B	7	Syringetin-3-O-galactoside	20.16	36.10	508.12	507.1	345	[19]: 345
E	8	Catechin	20.16	27.42	290.08	289.1	245, 203, $[2M-H]^-$: 579	[19,56–59]: 245 [19]: 203 [56]: 579
F	9	Gallic acid	21.12	18.34	170.02	169.0		
B	10	Syringetin-3-O-glucoside	23.04	38.81	508.12	507.1	345	[19]: 345
H	11	Procyanidin dimer	25.92	25.92	578.14	577.0	425	[13,56,58]: 425
B	12	Isorhamnetin-3-O-galactoside	25.92	37.66	478.11	477.3	447, 315, 314,	[19]: 447, 314, 315 [56,57]: 315
B	12	Isorhamnetin-3-O-glucoside	26.88	38.08	478.11	477.3	447, 314, 315	[19]: 447, 314, 315 [56,57]: 315
B	13	Laricitrin-3-O-galactoside/glucoside	26.88	35.52	494.11	493.1	330	[19]: 330
H	14	Procyanidin dimer	26.88	28.65	578.14	576.9	425	[13,56,58]: 425, 289
B	15	Myricetin-3-O-galactoside/glucoside	27.84	32.38	480.09	479.1	316	[19,55]: 316
B	16	Quercetin-3-O-glucoside /galactoside	27.84	34.84	464.1	463.1	301, 300	[58]: 301 [19,53–55]: 300 [53,56]: 179 [19] 163
H	17	Procyanidin dimer	28.80	25.62	578.14	577.0	425, 289	[13,56,58]: 425, 289
G	18	p-coumaric acid	29.76	33.79	164.05	163.0	119	[19]: 119
G	19	Caffeic acid	30.72	29.55	180.04	179.1	135	[19,58]: 135

C	20	Dihydro-quercetin	33.60	36.35	304.06	303.0	285, 125	[19,58]: 285, 125
C	21	Dihydro-kaempferol	39.36	40.39	288.06	287.1		
B	22	Myricetin-3-O rhamnoside*	41.28	34.71	464.09	463.1	317, 316	[60]: 317
B	23	Quercetin-3-O-rhamnoside*	47.04	38.00	448.10	447.1	301, 300, 271	[57,58]: 301 [54]: 300, 271 [55]: 271
B	24	Kaempferol-3-O-rhamnoside*	49.92	40.72	432.11	431.1	285	[41][64]: 431
B	25	Quercetin-3-O-acetyl-glucoside	59.52	40.74	506.11	505.0	301, 300	
C	26	Dihydro-laricitrin	68.16	35.36	334.07	333.1		
D	27	cis-/trans-Resveratrol	72.00	46.14	228.08	227.2		
D	28	cis-/trans-Resveratrol	82.56	46.16	228.08	227.2		
A	29	Syringetin	111.02	51.24	346.07	345.2	315	[19]: 315
A	30	Isorhamnetin	118.08	51.44	316.06	315.2	301, 300, 271	[63]: 301 [56]: 300 [19]: 271
A	31	Kaempferol	125.76	49.99	286.05	285.1		
A	32	Laricitrin	129.91	45.26	332.05	331.1	316, 179	[19]: 316, 179
A	33	Quercetin	130.56	45.24	302.04	301.2	179, 151, $[2M-H]^-$: 603	[13,19,53,56,58,61,62]: 179, 151
A	34	Myricetin	131.52	39.91	318.04	317.1	179, 151, 137	[19,56,62] : 137 [19,56,58,62]: 179, 151

* Neutral loss of m/z 146 implies the sugar moiety is a deoxyhexose, most likely rhamnose

The elution order of flavonoid aglycones in RPLC follows the expected order: flavanols < flavanones < flavonols < flavones [37,65,66]. This is influenced by the hydrophobicity of the molecules, determined by the number of methoxy substituents or adversely affected by the number of hydroxyl groups, as confirmed here for the flavanols and flavonols found.

The elution order for glycosylated flavonoids in RPLC follows the trend: galactosides < glucosides < arabinosides < xylosides < rhamnosides [37]. In accordance with literature, in the present work, flavonol-glucoside and/or –galactoside as well as –rhamnoside species were detected in the wine extract. The flavonol-hexoside isomers containing glucoside and galactoside moieties could not be differentiated based on the available MS data, except in instances where they are chromatographically resolved, where the known RPLC elution order (galactoside < glucoside) could be used to tentatively assign them. In this case two signals were found for Isorhamnetin-galactoside and -glucoside and Syringetin-galactoside and -glucoside. Based on the usual elution order, it is assumed that the later eluting analyte corresponds to the glucoside variant. Flavonols, most abundant in the berry skins, provide relatively selective absorption at 360 nm (since anthocyanins are not present in the ether extracts); Figure 3c shows the selective contour plot obtained at this wavelength for the wine sample.

The hydroxybenzoic and hydroxycinnamic acids were mostly detected in free as opposed to esterified forms, with the exception of fertaric acid, the tartaric acid ester of ferulic acid. One of the most abundant and well-known stilbenes, trans-resveratrol [37], was also detected in the wine extract, together with its cis-isomer as two signals for m/z 227 were found. Interestingly, while these isomers could not be separated in the short 2D RPLC gradient, they were well resolved in the TRLC dimension. Resveratrol-glucoside, piceid, was also identified based on its MS spectral data.

The general elution order of the compound classes in TRLC seems to be flavanols and hydroxybenzoic acids, followed by flavonol-glycosides and hydroxycinnamic acids, dihydroflavonols, the aglycone stilbenes and finally the aglycone flavonols, which are highly retained on the TRLC phase. This was further confirmed with the available standards, supporting the compound identification through MS. While the elution order of TRLC does show some correlation compared to RPLC, as both are based on hydrophobicity, good distribution of the analyte peaks in the two-dimensional space is nevertheless obtained.

The group-type separation of the wine phenolics is demonstrated in Figure 4, which shows the normalized retention times for selected compounds in TRLC×RPLC. To get a better impression of the selectivity differences between TRLC×RPLC and HILIC×RPLC, a common LC×LC configuration used for phenolic analysis, values for the same compounds taken with permission from Muller et al. [19] are shown in Figure 4b. In both studies a young South African red wine extract was analyzed, using the same RP column in the ^{2}D. Furthermore, the ^{2}D mobile phases and gradients are similar between these studies, albeit with slight differences in the time-dependent shifts in the gradient, making the gradient a little shallower for the TRLC×RPLC analysis. The major difference between Figure 4a and b is therefore due to the separation mode used in the first dimension, which gives an indication of the selectivity differences of TRLC and HILIC for the same phenolic compounds. HILIC×RPLC is popular for phenolic analysis due to the high orthogonality of this combination and its ability to provide group-type separation. This is evident in Figure 4b, where compound classes elute in the same vicinity, although with some overlap. Retention in HILIC increases with increasing glycosylation, while RPLC separates molecules based on the type of sugar (e.g. flavonols) [13]. Similarly, the TRLC×RPLC separation also shows grouping of the phenolic compound classes, although in different sequence and regions. In general, better separation of the apolar constituents (stilbenes and flavonol aglycones) from other phenolic classes is observed in TRLC×RPLC, whereas more polar glycosylated and acidic compound classes overlap somewhat in the earlier retention window. In this case, the flavonol aglycones elute as the last compound group – these show the strongest temperature-responsive effect in combination with the reversed temperature gradient used here, as presented in the Van't Hoff plot earlier. However, complete separation of the free flavonols and their glycosylated forms is relatively challenging for all three separation modes, demonstrating the benefit gained here by the two-dimensional separation.

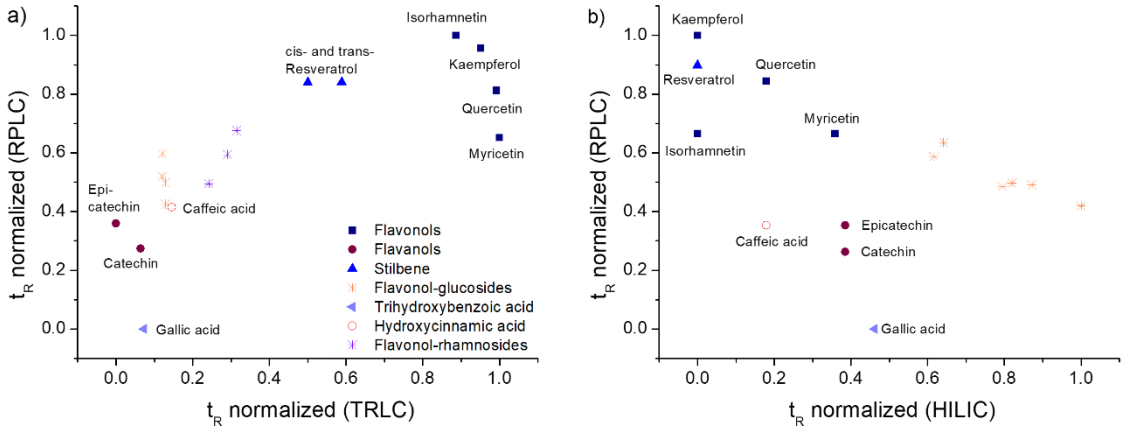

Figure 4: Plots of the normalized retention times ($t_{R,\,1D}$ / $t_{R,\,2D}$) taken from contour plots of selected phenolic compounds obtained for the analysis of young red wines by TRLC×RPLC and HILIC×RPLC. a) TRLC×RPLC analysis: TRLC in the ^{1}D (100x2.1 mm, 5 µm; reverse temperature gradient) and RPLC in the ^{2}D (Zorbax Eclipse Plus 50×3mm, 1.8 µm; fixed solvent gradient); b) HILIC×RPLC analysis, values taken with permission from Muller et. al. [19], using HILIC in the ^{1}D (Xbridge Amide column (150×1.0 mm, 1.7 µm, Waters; solvent gradient) and RPLC in the ^{2}D (Zorbax Eclipse Plus 50×3mm, 1.8 µm; fixed solvent gradient).

To estimate the orthogonality of the TRLC×RPLC combination, the Asterisk method [67] was used, providing a value of 65% for A_0 for the wine sample; this is very similar to the A_0 of 66% reported for HILIC×RPLC in [19]. The fractional surface coverage, here calculated following the convex hull method [68], was 52% for the TRLC×RPLC separation, again similar to 59% for HILIC×RPLC [19] (S7). This indicates that despite the similarities in selectivity between TRLC and RPLC for phenolics based on hydrophobicity, good exploitation of the two-dimensional space can be achieved for this combination. This may be partly ascribed to selectivity differences for hydrophobic molecules with additional hydroxyl groups, which are highly retained in TRLC at temperatures above the LCST, as shown in the van't Hoff plot and Figure 2.

Our findings therefore indicate the suitability of the in-house produced TR columns used in TRLC×RPLC for the facile 2D-LC analysis of phenolic compounds as a complementary LC×LC technique in the field of phenolic analysis. The implementation of TRLC does not add instrumental complexity as temperature programming is possible with common air-driven column thermostats, as e.g. used to heat up the ^{2}D column, allowing for traceable data collection with standard software. Further improvement in the methodology can however be realized. While the relatively generic RPLC gradient used in the ^{2}D in the present work led to acceptable separation of the wine phenolics, further improvements may be obtained by using shifted gradients or parallel gradients, which show particular benefit for partially correlated separation systems such as TRLC×RPLC [69]. Furthermore, improvements in the temperature gradient used for TRLC should prove beneficial. The temperature gradient used here in the first dimension was successful in decreasing retention for highly retained compounds but leaves room for improvement regarding the efficiency of temperature transfer between the system and the column. In the present work, the effective temperature gradients are rather slow, and further hindered by the low flow rates applied in the first dimension. This leads to long measurement times, thus limiting the achievable peak capacity rates to values lower than alternative LC×LC approaches. For example, practical peak capacities corrected for undersampling and finite surface coverage of around 1300 were reported for HILIC×RPLC separation of wine phenolics in an analysis time of an hour [19]. For the TRLC×RPLC method used here, a practical peak capacity corrected for undersampling and fractional surface coverage of 850 was obtained for an analysis time of two hours. This nevertheless represented a drastic improvement in comparison to earlier TRLC×RPLC work [23,24].

4. Conclusions

In this work, TRLC×RPLC combined with photodiode array and mass spectrometry detection was for the first time applied for the analysis of natural product extracts. Satisfactory separation was obtained for red wine phenolic extracts with the presented TRLC×RPLC set-up in comparison to other state-of-the-art LC×LC separations, with much less complicated method development. TRLC×RPLC provided at least partial group-type separation, especially prominent for flavonols, which show strong temperature-dependent behavior. The approach generally appears to allow for sensitive detection and identification of phenolic solutes, which can be further improved using high resolution MS instrumentation. The complexity of the samples and the possibilities of the technique are further highlighted through the TRLC×RPLC-DAD data.

5. Acknowledgments

The authors would like to thank Agilent Technologies for providing the LC×LC instrumentation, reversed-phase columns, and fruitful advice. The FWO is gratefully acknowledged for funding part of this research through the bilateral Belgium-South Africa Research Grant from FWO Vlaanderen (G0G8817N). Part of the research leading

to these results also received funding from the European Union's EU Framework Programme for Research and Innovation Horizon 2020 under Grant Agreement No 861369 (MSCA-ETN InnovEOX).

6. References

[1] B.W.J. Pirok, A.F.G. Gargano, P.J. Schoenmakers, Optimizing separations in online comprehensive two-dimensional liquid chromatography, J. Sep. Sci. 41 (2018) 68–98. https://doi.org/10.1002/jssc.201700863.

[2] G. Vanhoenacker, P. Sandra, Elevated temperature and temperature programming in conventional liquid chromatography - Fundamentals and applications, J. Sep. Sci. 29 (2006) 1822–1835. https://doi.org/10.1002/jssc.200600160.

[3] P. Sandra, G. Vanhoenacker, Elevated temperature-extended column length conventional liquid chromatography to increase peak capacity for the analysis of tryptic digests, J. Sep. Sci. 30 (2007) 241–244. https://doi.org/10.1002/jssc.200600329.

[4] F. Lestremau, A. de Villiers, F. Lynen, A. Cooper, R. Szucs, P. Sandra, High efficiency liquid chromatography on conventional columns and instrumentation by using temperature as a variable: Kinetic plots and experimental verification, J. Chromatogr. A. 1138 (2007) 120–131. https://doi.org/10.1016/J.CHROMA.2006.10.042.

[5] I. François, K. Sandra, P. Sandra, Comprehensive liquid chromatography: Fundamental aspects and practical considerations—A review, Anal. Chim. Acta. 641 (2009) 14–31. https://doi.org/10.1016/J.ACA.2009.03.041.

[6] F. Cacciola, K. Arena, F. Mandolfino, D. Donnarumma, P. Dugo, L. Mondello, Reversed phase versus hydrophilic interaction liquid chromatography as first dimension of comprehensive two-dimensional liquid chromatography systems for the elucidation of the polyphenolic content of food and natural products, J. Chromatogr. A. 1645 (2021) 462129. https://doi.org/10.1016/J.CHROMA.2021.462129.

[7] F. Erni, R.W. Frei, Two-dimensional column liquid chromatographic technique for resolution of complex mixtures, J. Chromatogr. A. 149 (1978) 561–569. https://doi.org/10.1016/S0021-9673(00)81011-0.

[8] D.R. Stoll, Recent advances in 2D-LC for bioanalysis, Bioanalysis. 7 (2015) 3125–3142. https://doi.org/10.4155/bio.15.223.

[9] Y. Chen, L. Montero, O.J. Schmitz, Advance in on-line two-dimensional liquid chromatography modulation technology, TrAC - Trends Anal. Chem. 120 (2019) 115647. https://doi.org/10.1016/j.trac.2019.115647.

[10] D. Li, O.J. Schmitz, Use of shift gradient in the second dimension to improve the separation space in comprehensive two-dimensional liquid chromatography, Anal. Bioanal. Chem. 405 (2013) 6511–6517. https://doi.org/10.1007/s00216-013-7089-5.

[11] D.R. Stoll, X. Li, X. Wang, P.W. Carr, S.E.G. Porter, S.C. Rutan, Fast, comprehensive two-dimensional liquid chromatography, J. Chromatogr. A. 1168 (2007) 3–43. https://doi.org/10.1016/j.chroma.2007.08.054.

[12] K.M. Kalili, A. De Villiers, Systematic optimisation and evaluation of on-line, off-line and stop-flow comprehensive hydrophilic interaction chromatography × reversed phase liquid chromatographic analysis of procyanidins, Part I: Theoretical considerations, J. Chromatogr. A. 1289 (2013) 58–68. https://doi.org/10.1016/j.chroma.2013.03.008.

[13] K.M. Kalili, A. De Villiers, Off-line comprehensive two-dimensional hydrophilic interaction × reversed phase liquid chromatographic analysis of green tea phenolics, J. Sep. Sci. 33 (2010) 853–863. https://doi.org/10.1002/jssc.200900673.

[14] B.W.J. Pirok, D.R. Stoll, P.J. Schoenmakers, Recent Developments in Two-Dimensional Liquid Chromatography: Fundamental Improvements for Practical Applications, Anal. Chem. 91 (2019) 240–

263. https://doi.org/10.1021/acs.analchem.8b04841.

[15] D.R. Stoll, K. Shoykhet, P. Petersson, S. Buckenmaier, Active Solvent Modulation: A Valve-Based Approach to Improve Separation Compatibility in Two-Dimensional Liquid Chromatography, Anal. Chem. 89 (2017) 9260–9267. https://doi.org/10.1021/acs.analchem.7b02046.

[16] P. Dugo, O. Favoino, R. Luppino, G. Dugo, L. Mondello, Comprehensive Two-Dimensional Normal-Phase (Adsorption)-Reversed-Phase Liquid Chromatography, Anal. Chem. 76 (2004) 2525–2530. https://doi.org/10.1021/ac0352981.

[17] P. Donato, F. Rigano, F. Cacciola, M. Schure, S. Farnetti, M. Russo, P. Dugo, L. Mondello, Comprehensive two-dimensional liquid chromatography–tandem mass spectrometry for the simultaneous determination of wine polyphenols and target contaminants, J. Chromatogr. A. 1458 (2016) 54–62. https://doi.org/10.1016/j.chroma.2016.06.042.

[18] M.R. Filgueira, Y. Huang, K. Witt, C. Castells, P.W. Carr, Improving peak capacity in fast online comprehensive two-dimensional liquid chromatography with post-first-dimension flow splitting, Anal. Chem. 83 (2011) 9531–9539. https://doi.org/10.1021/AC202317M.

[19] M. Muller, A.G.J. Tredoux, A. de Villiers, Application of Kinetically Optimised Online HILIC × RP-LC Methods Hyphenated to High Resolution MS for the Analysis of Natural Phenolics, Chromatographia. 82 (2019) 181–196. https://doi.org/10.1007/s10337-018-3662-6.

[20] Q. Li, F. Lynen, J. Wang, H. Li, G. Xu, P. Sandra, Comprehensive hydrophilic interaction and ion-pair reversed-phase liquid chromatography for analysis of di- to deca-oligonucleotides, J. Chromatogr. A. 1255 (2012) 237–243. https://doi.org/10.1016/J.CHROMA.2011.11.062.

[21] H. Tian, J. Xu, Y. Xu, Y. Guan, Multidimensional liquid chromatography system with an innovative solvent evaporation interface, J. Chromatogr. A. 1137 (2006) 42–48. https://doi.org/10.1016/J.CHROMA.2006.10.005.

[22] K. Horváth, J.N. Fairchild, G. Guiochon, Detection issues in two-dimensional on-line chromatography, J. Chromatogr. A. 1216 (2009) 7785–7792. https://doi.org/10.1016/j.chroma.2009.09.016.

[23] M. Baert, S. Martens, G. Desmet, A.J. de Villiers, F.E. Du Prez, F. Lynen, Enhancing the possibilities of comprehensive two-dimensional liquid chromatography through hyphenation of purely aqueous temperature-responsive and reversed-phase liquid chromatography, Anal. Chem. 90 (2018) 4961–4967. https://doi.org/10.1021/acs.analchem.7b04914.

[24] K. Wicht, M. Baert, A. Kajtazi, S. Schipperges, N. von Doehren, G. Desmet, A. de Villiers, F. Lynen, Pharmaceutical impurity analysis by comprehensive two-dimensional temperature responsive × reversed phase liquid chromatography, J. Chromatogr. A. 1630 (2020) 461561. https://doi.org/10.1016/j.chroma.2020.461561.

[25] F. Lynen, J.M.D. Heijl, F.E. Du Prez, R. Brown, R. Szucs, P. Sandra, Evaluation of the temperature responsive stationary phase poly (N-isopropylacrylamide) in aqueous LC for the analysis of small molecules, Chromatographia. 66 (2007) 143–150. https://doi.org/10.1365/s10337-007-0301-z.

[26] H. Kanazawa, Y. Kashiwase, K. Yamamoto, Y. Matsushima, A. Kikuchi, Y. Sakurai, T. Okano, Temperature-Responsive Liquid Chromatography. 2. Effects of Hydrophobic Groups in *N* -Isopropylacrylamide Copolymer-Modified Silica, Anal. Chem. 69 (1997) 823–830. https://doi.org/10.1021/ac961024k.

[27] M. Baert, K. Wicht, Z. Hou, R. Szucs, F. Du Prez, F. Lynen, Exploration of the Selectivity and Retention Behavior of Alternative Polyacrylamides in Temperature Responsive Liquid Chromatography, Anal. Chem. 92 (2020) 9815–9822. https://doi.org/10.1021/acs.analchem.0c01321.

[28] E. Ayano, H. Kanazawa, Aqueous chromatography system using temperature-responsive polymer-modified stationary phases., J. Sep. Sci. 29 (2006) 738–749. https://doi.org/10.1002/jssc.200500485.

[29] R. Hoogenboom, Temperature-responsive polymers: Properties, synthesis and applications, Woodhead

Publishing Limited, 2014. https://doi.org/10.1533/9780857097026.1.15.

[30] H. Kanazawa, Y. Matsushima, T. Okano, Temperature-responsive chromatography, TrAC - Trends Anal. Chem. 17 (1998) 435–440. https://doi.org/10.1016/S0165-9936(98)00044-2.

[31] A.J. Satti, P. Espeel, S. Martens, T. Van Hoeylandt, F.E. Du Prez, F. Lynen, Tunable temperature responsive liquid chromatography through thiolactone-based immobilization of poly(N-isopropylacrylamide), J. Chromatogr. A. 1426 (2015) 126–132. https://doi.org/10.1016/J.CHROMA.2015.11.063.

[32] B. Miserez, F. Lynen, A. Wright, M. Euerby, P. Sandra, Thermoresponsive Poly(N-vinylcaprolactam) as Stationary Phase for Aqueous and Green Liquid Chromatography, Chromatographia. 71 (2010) 1–6. https://doi.org/10.1365/s10337-009-1394-3.

[33] E. Ayano, Y. Okada, C. Sakamoto, H. Kanazawa, T. Okano, M. Ando, T. Nishimura, Analysis of herbicides in water using temperature-responsive chromatography and an aqueous mobile phase., J. Chromatogr. A. 1069 (2005) 281–5. http://www.ncbi.nlm.nih.gov/pubmed/15830956 (accessed March 27, 2018).

[34] H. Kanazawa, M. Nishikawa, A. Mizutani, C. Sakamoto, Y. Morita-Murase, Y. Nagata, A. Kikuchi, T. Okano, Aqueous chromatographic system for separation of biomolecules using thermoresponsive polymer modified stationary phase, J. Chromatogr. A. 1191 (2008) 157–161. https://doi.org/10.1016/J.CHROMA.2008.01.056.

[35] T. Mikuma, R. Uchida, M. Kajiya, Y. Hiruta, H. Kanazawa, The use of a temperature-responsive column for the direct analysis of drugs in serum by two-dimensional heart-cutting liquid chromatography, Anal. Bioanal. Chem. 409 (2017) 1059–1065. https://doi.org/10.1007/s00216-016-0024-9.

[36] K.M. Kalili, A. de Villiers, Recent developments in the HPLC separation of phenolic compounds, J. Sep. Sci. 34 (2011) 854–876. https://doi.org/10.1002/jssc.201000811.

[37] A. De Villiers, P. Venter, H. Pasch, Recent advances and trends in the liquid-chromatography – mass spectrometry analysis of flavonoids, J. Chromatogr. A. 1430 (2016) 16–78. https://doi.org/10.1016/j.chroma.2015.11.077.

[38] M. Saltmarsh, C. Santos-Buelga, G. Williamson, Methods in Polyphenol Analysis, 2003. https://pubs.rsc.org/en/content/ebook/978-0-85404-580-8.

[39] D.V. Ratnam, D.D. Ankola, V. Bhardwaj, D.K. Sahana, M.N.V.R. Kumar, Role of antioxidants in prophylaxis and therapy: A pharmaceutical perspective, J. Control. Release. 113 (2006) 189–207. https://doi.org/10.1016/j.jconrel.2006.04.015.

[40] J.Q. Wu, T.R. Kosten, X.Y. Zhang, Free radicals, antioxidant defense systems, and schizophrenia, Prog. Neuro-Psychopharmacology Biol. Psychiatry. 46 (2013) 200–206. https://doi.org/10.1016/j.pnpbp.2013.02.015.

[41] E. Ruszová, J. Cheel, S. Pávek, M. Moravcová, M. Hermannová, I. Matějková, J. Velebný, S. Vladimír, L. Kubala, Epilobium angustifolium extract demonstrates multiple effects on dermal fibroblasts in vitro and skin photo-protection in vivo, Gen. Physiol. Biophys. 32 (2013) 347–359. https://doi.org/10.4149/gpb_2013031.

[42] M. Martorana, T. Arcoraci, L. Rizza, M. Cristani, F.P. Bonina, A. Saija, D. Trombetta, A. Tomaino, In vitro antioxidant and in vivo photoprotective effect of pistachio (Pistacia vera L., variety Bronte) seed and skin extracts, Fitoterapia. 85 (2013) 41–48. https://doi.org/10.1016/j.fitote.2012.12.032.

[43] P. Lucci, J. Saurina, O. Núñez, Trends in LC-MS and LC-HRMS analysis and characterization of polyphenols in food, TrAC - Trends Anal. Chem. 88 (2017) 1–24. https://doi.org/10.1016/j.trac.2016.12.006.

[44] R. Blomhoff, Dietary antioxidants and cardiovascular disease, Curr. Opin. Lipidol. 16 (2005) 47–54. https://doi.org/10.1016/s1566-3124(02)11037-6.

[45] N.A. Walters, A. de Villiers, E. Joubert, D. de Beer, Phenolic profiling of rooibos using off-line comprehensive normal phase countercurrent chromatography × reversed phase liquid chromatography, J. Chromatogr. A. 1490 (2017) 102–114. https://doi.org/10.1016/j.chroma.2017.02.021.

[46] C.M. Willemse, M.A. Stander, J. Vestner, A.G.J. Tredoux, A. De Villiers, Comprehensive Two-Dimensional Hydrophilic Interaction Chromatography (HILIC) × Reversed-Phase Liquid Chromatography Coupled to High-Resolution Mass Spectrometry (RP-LC-UV-MS) Analysis of Anthocyanins and Derived Pigments in Red Wine, Anal. Chem. 87 (2015) 12006–12015. https://doi.org/10.1021/acs.analchem.5b03615.

[47] E. Sommella, O.H. Ismail, F. Pagano, G. Pepe, C. Ostacolo, G. Mazzoccanti, M. Russo, E. Novellino, F. Gasparrini, P. Campiglia, Development of an improved online comprehensive hydrophilic interaction chromatography ×reversed-phase ultra-high-pressure liquid chromatography platform for complex multiclass polyphenolic sample analysis, J. Sep. Sci. 40 (2017) 2188–2197. https://doi.org/10.1002/jssc.201700134.

[48] F. Cacciola, P. Jandera, Z. Hajdú, P. Česla, L. Mondello, Comprehensive two-dimensional liquid chromatography with parallel gradients for separation of phenolic and flavone antioxidants, J. Chromatogr. A. 1149 (2007) 73–87. https://doi.org/10.1016/j.chroma.2007.01.119.

[49] S. Peters, G. Vivó-Truyols, P.J. Marriott, P.J. Schoenmakers, Development of an algorithm for peak detection in comprehensive two-dimensional chromatography, J. Chromatogr. A. 1156 (2007) 14–24. https://doi.org/10.1016/j.chroma.2006.10.066.

[50] A. Moussa, T. Lauer, D. Stoll, G. Desmet, K. Broeckhoven, Numerical and experimental investigation of analyte breakthrough from sampling loops used for multi-dimensional liquid chromatography, J. Chromatogr. A. 1626 (2020) 461283. https://doi.org/10.1016/j.chroma.2020.461283.

[51] L.-Z. Lin, J.M. Harnly, Quantitation of Flavanols, Proanthocyanidins, Isoflavones, Flavanones, Dihydrochalcones, Stilbenes, Benzoic Acid Derivatives Using Ultraviolet Absorbance after Identification by Liquid Chromatography–Mass Spectrometry, J. Agric. Food Chem. 60 (2012) 5832. https://doi.org/10.1021/JF3006905.

[52] V. Gavrilova, M. Kajdžanoska, V. Gjamovski, M. Stefova, Separation, characterization and quantification of phenolic compounds in blueberries and red and black currants by HPLC-DAD-ESI-MSn, J. Agric. Food Chem. 59 (2011) 4009–4018. https://doi.org/10.1021/jf104565y.

[53] Z.-H. Li, H. Guo, W.-B. Xu, J. Ge, X. Li, M. Alimu, D.-J. He, Rapid Identification of Flavonoid Constituents Directly from PTP1B Inhibitive Extract of Raspberry (Rubus idaeus L.) Leaves by HPLC–ESI–QTOF–MS-MS, J. Chromatogr. Sci. 54 (2016) 805. https://doi.org/10.1093/CHROMSCI/BMW016.

[54] A. Li, X. Hou, Y. Wei, Fast screening of flavonoids from switchgrass and: Mikania micrantha by liquid chromatography hybrid-ion trap time-of-flight mass spectrometry, Anal. Methods. 10 (2018) 109–122. https://doi.org/10.1039/c7ay02103h.

[55] A.P. Singh, Y. Wang, R.M. Olson, D. Luthria, G.S. Banuelos, S. Pasakdee, N. Vorsa, T. Wilson, LC-MS-MS Analysis and the Antioxidant Activity of Flavonoids from Eggplant Skins Grown in Organic and Conventional Environments, Food Nutr. Sci. 08 (2017) 873–888. https://doi.org/10.4236/FNS.2017.89063.

[56] G.L. La Torre, M. Saitta, F. Vilasi, T. Pellicanò, G. Dugo, Direct determination of phenolic compounds in Sicilian wines by liquid chromatography with PDA and MS detection, Food Chem. 94 (2006) 640–650. https://doi.org/10.1016/J.FOODCHEM.2005.02.007.

[57] E. Sommella, G. Pepe, F. Pagano, C. Ostacolo, G.C. Tenore, M.T. Russo, E. Novellino, M. Manfra, P. Campiglia, Detailed polyphenolic profiling of Annurca apple (M. pumila Miller cv Annurca) by a combination of RP-UHPLC and HILIC, both hyphenated to IT-TOF mass spectrometry, Food Res. Int. 76 (2015) 466–477. https://doi.org/10.1016/j.foodres.2015.05.044.

[58] J. Sun, F. Liang, Y. Bin, P. Li, C. Duan, Screening non-colored phenolics in red wines using liquid chromatography/ultraviolet and mass spectrometry/mass spectrometry libraries, Molecules. 12 (2007) 679–693. https://doi.org/10.3390/12030679.

[59] E. Akyuz, H. Şahin, F. Islamoglu, S. Kolayli, P. Sandra, H. Huseyin¸ Huseyin¸sahin, Evaluation of Phenolic Compounds in Tilia rubra Subsp. caucasica by HPLC-UV and HPLC-UV-MS/MS, Int. J. Food Prop. 17 (2014) 331–343. https://doi.org/10.1080/10942912.2011.631252.

[60] L.L. Saldanha, W. Vilegas, A.L. Dokkedal, Characterization of Flavonoids and Phenolic Acids in Myrcia bella Cambess. Using FIA-ESI-IT-MSn and HPLC-PAD-ESI-IT-MS Combined with NMR, Molecules. 18 (2013) 8402. https://doi.org/10.3390/MOLECULES18078402.

[61] A. Brito, J.E. Ramirez, C. Areche, B. Sepúlveda, M.J. Simirgiotis, HPLC-UV-MS Profiles of Phenolic Compounds and Antioxidant Activity of Fruits from Three Citrus Species Consumed in Northern Chile, Molecules. 19 (2014) 17400–17421. https://doi.org/10.3390/molecules191117400.

[62] G. Vanhoenacker, A. De Villiers, K. Lazou, D. De Keukeleire, P. Sandra, Comparison of high-performance liquid chromatography — Mass spectroscopy and capillary electrophoresis— mass spectroscopy for the analysis of phenolic compounds in diethyl ether extracts of red wines, Chromatographia. 54 (2001) 309–315. https://doi.org/10.1007/BF02492675.

[63] M. Sobeh, E. ElHawary, H. Peixoto, R.M. Labib, H. Handoussa, N. Swilam, A.H. El-Khatib, F. Sharapov, T. Mohamed, S. Krstin, M.W. Linscheid, A.N. Singab, M. Wink, N. Ayoub, Identification of phenolic secondary metabolites from Schotia brachypetala Sond. (Fabaceae) and demonstration of their antioxidant activities in Caenorhabditis elegans, PeerJ. 2016 (2016). https://doi.org/10.7717/peerj.2404.

[64] †,‡ Sari Ek, † Heikki Kartimo, † and Sampo Mattila, †,‡ Ari Tolonen*, Characterization of Phenolic Compounds from Lingonberry (Vaccinium vitis-idaea), J. Agric. Food Chem. 54 (2006) 9834–9842. https://doi.org/10.1021/JF0623687.

[65] B. Abad-García, L.A. Berrueta, S. Garmón-Lobato, B. Gallo, F. Vicente, A general analytical strategy for the characterization of phenolic compounds in fruit juices by high-performance liquid chromatography with diode array detection coupled to electrospray ionization and triple quadrupole mass spectrometry, J. Chromatogr. A. 1216 (2009) 5398–5415. https://doi.org/10.1016/j.chroma.2009.05.039.

[66] H. Sakakibara, Y. Honda, S. Nakagawa, H. Ashida, K. Kanazawa, Simultaneous determination of all polyphenols in vegetables, fruits, and teas, J. Agric. Food Chem. 51 (2003) 571–581. https://doi.org/10.1021/jf020926l.

[67] M. Camenzuli, P.J. Schoenmakers, A new measure of orthogonality for multi-dimensional chromatography, Anal. Chim. Acta. 838 (2014) 93–101. https://doi.org/10.1016/j.aca.2014.05.048.

[68] G. Semard, V. Peulon-Agasse, A. Bruchet, J.P. Bouillon, P. Cardinaël, Convex hull: A new method to determine the separation space used and to optimize operating conditions for comprehensive two-dimensional gas chromatography, J. Chromatogr. A. 1217 (2010) 5449–5454. https://doi.org/10.1016/j.chroma.2010.06.048.

[69] A.A. Aly, M. Muller, A. De Villiers, B.W.J. Pirok, T. Górecki, Parallel gradients in comprehensive multidimensional liquid chromatography enhance utilization of the separation space and the degree of orthogonality when the separation mechanisms are correlated, J. Chromatogr. A. 1628 (2020) 461452. https://doi.org/10.1016/j.chroma.2020.461452.